ASTFE American Society of Thermal and Fluids Engineers

10th Thermal and Fluids Engineering Conference (TFEC)
March 9-12, 2025
Partially Online Virtual and at George Washington University, Washington, DC Conference

TFEC-2025-55546

COMPUTATIONAL FLUID DYNAMICS MODEL OF HEAT TRANSFER IN THE VICINITY OF PHOTOVOLTAIC PANELS

Scott C. Vanderlan[1*], Ahmad Vasel-Be-Hagh[2], Jie Cui[1]

[1]Tennessee Technological University, Cookeville, TN 38505, USA
[2]University of South Florida, Tampa, FL 33620, USA

ABSTRACT

With a global push to lower carbon emissions, low-carbon solutions for electricity have grown in popularity. However, industrial-scale photovoltaic (PV) panel projects require large areas of land, increasing the installed global PV plant area beyond several hundred million acres. Could a change this large affect the local climate? Answering this question requires a clear understanding of processes through which the PV panels can potentially affect the viscous sub-layer of the atmospheric boundary layer. It is also essential to understand the extent to which each process plays a role. Since doing so experimentally would be very challenging, using Computational Fluid Dynamics (CFD) models becomes inevitable. Such models have been used to simulate various physical aspects in the vicinity of PV panels for decades, typically focused on improving the system's design to enhance the performance of solar cells. However, there is a dearth of research focusing on increasing our understanding of the thermal and mechanical interactions between PV panels, the ground, and the air to reveal how the existence of these panels alters near-ground thermal characteristics. This paper shares our preliminary CFD model of a small scale PV system, which was built using Ansys Fluent. The simulation utilized turbulence, radiation, energy, and solar load models. It is shown that the model agrees well with our field-collected results, demonstrating its reliability and potential for providing a systematic parametric study. Therefore, the model could be used to study the surface heat fluxes in the system for differing conditions. Future work is planned to simulate the unique heat transfer mechanisms of a large solar farm, including daily temporal effects.

KEYWORDS: Computational Fluid Dynamics, Photovoltaic Panels, Radiation Heat Transfer

NOMENCLATURE

k	Turbulent kinetic energy (TKE)	(J/kg)	$C_{3\varepsilon}$	Variable $=tanh\|v/u\|$	(-)
ε	TKE dissipation rate	(W/kg)	G_b	Generation of TKE due to mean velocity gradients	
μ_t	Eddy viscosity	(m^2/s)			
σ_k	Constant = 1.0 (Pr for k)	(-)	G_k	Generation of TKE due to buoyancy	
σ_ε	Constant = 1.2 (Pr for ε)	(-)	n	Refractive index	(-)
Ω'	Solid angle	(rad)	S_ε	User defined source term	(-)
ω	TKE specific dissipation rate	(1/s)	S_k	User defined source term	(-)
C_1	Variable based on k/ε and rate-of-strain tensor		Y_M	Fluctuating dilation in compressible turbulence to the overall dissipation rate	
$C_{1\varepsilon}$	Constant = 1.44	(-)	y^+	non-dimensional wall distance	(-)
C_2	Constant = 1.9	(-)			

*Corresponding Author: scvanderla21@tntech.edu

1. INTRODUCTION AND BACKGROUND

The history of photovoltaic (PV) panels goes back to the mid-19th century when the first observation of photovoltaic effects in materials was made. The first demonstration of a commercially viable silicon-based PV panel was in 1954 [1]. This technology is the basis of today's industrial PV panels. However, it wasn't until the 21st century that industrial-scale electricity generation using PV panels became financially viable [2]. This was primarily due to improving PV panel efficiency and the construction cost, along with the development of new electronics, making it possible to add power from PV panels to the grid [3].

With a global push to lower carbon emissions, low-carbon solutions for electricity have grown in popularity. However, industrial-scale PV panel projects require large areas of land. The land area required varies by latitude, ranging from 2.5 acres per megawatt in the tropics to nearly 5 acres per megawatt in northern Europe [4]. There has been some contradictory research into the effects of PV power stations on local temperatures. Barron-Gafford et al. [5] suggest PV plants create a heat island, while Li et al. [6] suggest PV plants create a cool island effect. These studies use local temperature measurements to support the hypotheses. Both papers discuss the possible mechanisms responsible for the difference in temperatures with and without the PV plant canopy. Barron-Gafford found temperatures over a PV plant were regularly 3–4 ˚C warmer than wild-lands at night, which is in direct contrast to other studies based on models that suggested that PV systems should decrease ambient temperatures. Li suggests the cool island impact is attributable to the development of small-scale circulation cells, similar to those that develop around desert cities and water bodies.

Computational Fluid Dynamics (CFD) models have been used to simulate various physical aspects in the vicinity of PV panels for decades. This previous research is typically focused on improving the design of PV systems. Some research has used CFD to evaluate the extreme wind loads possible, ensuring the mounting systems are properly designed for these conditions [7,8,9,10]. Other studies focus on modeling the convective cooling effects, citing that efficiency degrades as the panels heat up as motivation [11,12,13]. There is a lack of investigations on how solar farms affect the surrounding environment, in particular, the thermal characteristics of the viscous sub-layer, i.e., nearly the first 10% of the atmospheric boundary layer. This article plans to address this by taking a preliminary step towards developing a CFD model to provide insight on the heat transfer phenomenon in the vicinity of the PV panel.

2. LITERATURE REVIEW

2.1 Wind Loading using CFD

A significant part of the literature concerning CFD analysis of PV solar farms focuses on analyzing the effects of high winds on PV panels. The difficulty of wind tunnel experiments for ground-mounted PV panels and arrays appears to be the primary motivation behind the extensive use of CFD for computing aerodynamic loads, in particular, the accurate recreation of the atmospheric boundary layer (ABL), velocity profiles, and turbulence conditions in such investigations [7,8].

The methodologies utilized for modeling turbulence in these studies are Reynolds Averaged Navier Stokes (RANS) models, particularly Shear Stress Transport (SST) k-ω [7,8,10] and Renormalization Group (RNG) k-ε [9]. Using commercially available codes such as Ansys Fluent [9,10] and open-source packages such as OpenFOAM [7,8] to implement these solutions appears to be common. Both transient [7,8,9] and steady state [10] models have been used. The length and number of time steps used for a transient simulation can vary from short time steps over 15 seconds of flow time [7,8] to only 1000 time steps for 2 seconds of flow time [9]. For either transient or steady state models, several parameters such as turbulence intensity and dissipation rates are evaluated to ensure proper representation of the turbulence conditions.

Since these simulations are for analyzing loads on the PV panels due to wind, a uniform free stream velocity profile can be used as an inlet condition when modeling long sections of wind tunnels because the sufficiently long interaction of airflow and the ground surface would cause the correct velocity profile to eventually form before wind goes over the panels since the geometry [9,10]. However, to use a smaller, more localized domain, a standard ABL velocity profile for flow along the ground must be set as the inlet condition [7,8]. The wind speeds used for these experiments are relatively high, ranging from 10 to 45 m/s, in order to simulate maximum load conditions. Wind tunnel experiments are often designed to be less than full-scale, depending on the wind tunnel size. Therefore, simulations of these types of experiments are modeled to the same scales [7,8,9].

For wind loading simulations, geometric parameters are often varied to find the maximum loading conditions. This can be done using only various wind directions [7,8], varying wind direction and tilt angles [9], or varying wind direction and the overall geometry of the PV panel systems [10]. In order to scientifically evaluate the results of these simulations, relevant parameters and coefficients are used for comparison. In these cases, the parameters reported are pressure, drag, and lift coefficients for the various conditions [7,8,9,10] along with pressure contour and streamline plots [9,10].

2.2 Convective Heat Transfer Studies using CFD

A number of articles exist in the literature that use CFD to analyze the convection heat transfer in the vicinity of PV panels. This line of research is motivated by improving PV performance at lower temperatures. Therefore, optimized designs will provide better cooling and, subsequently, better PV efficiency. Wind tunnel experiments often use a heated panel to simulate PV panels warmed by solar irradiation [11], others use scale models of rooftop-mounted or ducted PV panels to assess the flow fields and convective heat transfer [12,13]. These experiments have been modeled using open-source and commercial CFD software, including OpenFOAM [11], COMSOL Multi-Physics [12], and Ansys Fluent [13]. Similar to the previously reviewed articles, the RANS equations are solved using SST k-ω [11] and Standard k-ε [12,13] turbulence models.

One method to simulate natural and forced convective heat transfer in the vicinity of a PV panel in a wind tunnel, is by heating the model PV panel to some constant temperature and measuring the heat flux (cooling) at different wind speeds. This arrangement has been modeled using CFD with an additional solver added for the convection heat transfer calculations based on the Boussinesq approximation, which works for both natural and forced convection. In this case, the RANS equations are solved via pressure-velocity coupling using a Pressure Implicit with Splitting of Operators (PISO) algorithm [11]. The results of each simulation are used to calculate a convective heat transfer coefficient (CHTC) for each of the various initial conditions, including different wind speeds and directions [11]. The results are validated against wind tunnel experiments and demonstrate natural convection is dominant at lower wind speeds while forced convection is dominant at high wind speeds. The calculated CHTCs were compared to those determined by existing correlations of the coefficients from previous works [11].

The literature has also investigated how varying the geometry of the panels and surrounding structures affects velocities and flow fields around the panels [12]. Such studies have been also carried out using CFD and validated against wind tunnel experiments. The wind speeds used in the convective heat transfer experiments (typically between 1 and 5 meters per second) are less than the speeds used for wind loading investigations. It should be noted that most of the models reviewed above were set up as wind tunnel representations, with a velocity inlet and pressure outlet, both far from the test article with a “no-slip” condition for the ground wall and “slip” wall conditions for the sides and top.

A small part of the literature also includes CFD-based investigations aiming to model small-scale field experiments [13]. Often, boundary conditions are determined based on experimental results, in order to focus on certain concepts. For example, a hybrid photovoltaic thermal air collector, which is a PV panel with a duct beneath to collect heated air, which in turn cools the PV panel [14] was modelled [13]. In this case, a two-dimensional model, relying on several user-defined boundary conditions, is used to model all three

modes of heat transfer: radiation, conduction, and convection. The bottom of the panel was only subject to convective boundary conditions, and all other boundaries were adiabatic. This alludes to the capability being tested is the conduction through the modeled layers of the PV panel and the convective heat transfer to the air within the duct. The temperatures and efficiency calculations were compared to the experiment [13].

2.3 Radiation and Convective Heat Transfer using CFD

Only a few articles in the literature report on using CFD to model convection and radiation heat transfer around a PV panel simultaneously. Like the convection heat transfer articles reviewed in Section 2.2, the primary motivation of such studies appears to be enhancing PV panel performance by focusing on improving the cooling effects [15,16] and developing strategies to increase the incident radiation onto the PV panel [17]. To our knowledge, all these studies simulated radiation effects using the models available in Ansys Fluent. Only one considered simulating forced convection (wind). It used a Realizable k-ε turbulence model to simultaneously evaluate natural and forced convective heat transfer at various panel tilt angles and uniform free-stream wind velocities [15]. The others considered only natural convection with laminar flow [16] or only radiation heat transfer [17].

To develop a simulation that accounts for radiation heat transfer, one could use only the equations for energy [16], a radiation model [17], or both [15]. The Discrete Ordinates radiation model is the most efficient and often used. One of the reviewed articles used the solar loading feature in Fluent to set a normal solar angle with various values of solar based on measured experimental values [16]. Others used constant heat flux[15] or radiation boundary conditions[17] on the solid surfaces as input variables.

Though the motivation for improving performance is similar for these articles, the evaluation techniques differ. Some studies evaluate the average Nusselt number under various conditions as a representation of convective cooling capacity [15]. Also included, was a comparison of using constant heat flux or temperature-dependent heat flux as the input variable. The results were significantly different in most respects, but the Nusselt number was virtually the same, so the constant heat flux input was used for the study. Other studies have compared surface and air temperatures measured experimentally against the simulation results [16]. There are also studies that compared experimental and simulated incident radiation values [17].

In addition, the literature indicates ongoing efforts to develop models for construction materials [18,19,20]. These are mostly focused on improving the optical properties to improve performance. Some discuss the conductive properties of the materials of construction, with a focus on moving the excess heat away from the PV cells. Several articles were also reviewed to inform the setup of the model presented herein. These included properties of the soil [21,22,23].

3. MOTIVATION

The primary motivation stems from the significant growth of solar energy in response to CO_2 and other emissions of conventional fossil fuel power plants. While solar energy is an excellent and effective solution to such issues, it is necessary to investigate its potential non-CO_2 climate effects, such as a heat island effect [24], to ensure this essential and much-needed expansion occurs effectively so that the non-CO_2 emissions will have a minimal effect on the gains. An analogy to aviation's non-CO_2 emissions would help clarify this research's motivation. Aviation contributes to 2.5% of global CO_2 production. However, CO_2 generation makes up only one-third of this industry's climate effect, with two-thirds being from non-CO_2 emissions. The most major non-CO_2 emission of aviation is the radiative effect of the condensation trails, aka contrails, that appear as small clouds that form behind airplanes way up in the sky. Contrails affect the climate by interfering with incoming and outgoing radiative heat fluxes. Interestingly, while only a small fraction of flights occurs at night, most of the contrail effect belongs to those forming at nighttime. At night, there are no incoming solar fluxes, and the ground radiates the heat that was stored in it during the day back into

space. Contrails can block this one-way radiation, causing a major climate effect measured via Effective Radiative Forcing (ERF).

Given the current PV cell's efficiency, generating 1 MW of electrical power would require several acres of installed PV panels. Thus, several hundred million acres of installed PV panels will emerge by 2050 to reach the 70 TW goal. Since this is a much more extensive area than that of contrails while being installed much closer to the ground surface, it is reasonable to question whether such a huge installation of panels would interfere with nighttime outgoing radiative fluxes that are supposed to cool down the ground and the air temperature atop.

4. PURPOSE OF RESEARCH

What sets our research apart from those disseminated in literature to date, is the focus on the heat fluxes at the PV panel and the ground, primarily through radiation heat transfer. We would like to enhance our understanding of how solar farms could affect the thermal characteristics of the local ABL, particularly within the viscous sub-layer, i.e., nearly the first 1% of the ABL's thickness. The major mechanisms being researched have to do with how heat transfer between the ground and the atmosphere could change in the presence of PV panels.

The literature review provided good insight and background on modeling the effects of wind and, more importantly, turbulence in the vicinity of the panel. Both of these contribute to the overall temperature of the PV panel through convective cooling. The articles reviewed also provided many of the material properties of the components of the PV panels. However, in application, solar irradiation is the heat source for the panel and the ground. Additionally, radiation is the primary mode of heat transfer between the panel and the ground, and this interaction is not considered in the articles reviewed.

The interaction between solar radiation and the ground is a critical component of the stability of the ABL. Our research aims to evaluate how this interaction might change in the presence of a PV panel. One could consider, if the ground and the ABL are a system heated by solar radiation and cooled through natural or forced (wind) convection, how does the presence of a PV panel (or solar farm) affect that system? And how does the effect change when certain variables are considered? The research presented in this article is a preliminary step in developing CFD simulations that contribute to answering these questions.

5. SOLUTION

The initial model has been generated to duplicate the experimental setup used by Cannon & Vasel-Be-Hagh [25] to allow validation of the model against the experimental results. Several simulations will be run at different times throughout the day to compare to the experiment. This 3D CFD model has been constructed in Ansys Fluent to solve the momentum and energy equations using both turbulence and radiation models. The turbulence model is realizable k-ε, and the radiation model is Discrete Ordinates (DO).

The k-ε turbulence model was selected for its low computational cost, robustness, and reasonable accuracy. The realizable k-ε model differs from the standard k-ε model in two important ways. First, the realizable k-ε model contains an alternative formulation for the turbulent viscosity. Second, a modified transport equation for the dissipation rate (ε), has been derived from an exact equation for the transport of the mean-square vorticity fluctuation. The equations 1 and 2 below are used to solve for k and ε, respectively [26]. The term "realizable" means that the model satisfies certain mathematical constraints on the Reynolds stresses, consistent with the physics of turbulent flows [26]. This turbulence model has some sensitivities in the near wall regions so additional wall treatment calculations are employed. The preliminary model used the standard wall functions. However, other wall function options reduce sensitivities to y^+ and address model deficiencies at low Reynolds numbers.

$$\frac{\partial}{\partial t}(\rho k)+\frac{\partial}{\partial x_j}(\rho k u_j)=\frac{\partial}{\partial x_j}\left[\left(\mu+\frac{\mu_t}{\sigma_k}\right)\frac{\partial k}{\partial x_j}\right]+G_k+G_b-\rho\varepsilon-Y_M+S_k \quad (1)$$

$$\frac{\partial}{\partial t}(\rho \varepsilon)+\frac{\partial}{\partial x_j}(\rho \varepsilon u_j)=\frac{\partial}{\partial x_j}\left[\left(\mu+\frac{\mu_t}{\sigma_\varepsilon}\right)\frac{\partial \varepsilon}{\partial x_j}\right]+\rho C_1 S\varepsilon-\rho C_2\frac{\varepsilon^2}{k+\sqrt{\nu\varepsilon}}+C_{1\varepsilon}\frac{\varepsilon}{k}C_{3\varepsilon}G_b+S_\varepsilon \quad (2)$$

The DO radiation model was chosen for this application because it offers the most flexibility and accuracy at only a moderate computational cost. The DO model allows for any optical thickness, semi-transparent walls, and participating media. Some other advantages of the DO model are the ability to adjust the angular discretization or the use of non-gray radiation models defined by wavelength bands. Using a radiation model allows the option to apply a solar radiation input load based on the terrestrial location of the experimental setup by automatically adjusting irradiation values and incidence angles based on the time of day. This feature is crucial in analyzing the temporal changes in the system throughout the day. The DO radiation model considers the radiative transfer equation (RTE) in the direction $\vec{s}$ as a field function as shown in equation 3 [26].

$$\nabla\cdot\left(I(\vec{r},\vec{s})\vec{s}\right)+\left(a+\sigma_s\right)I(\vec{r},\vec{s})=an^2\frac{\sigma T^4}{\pi}+\frac{\sigma_s}{4\pi}\int_0^{4\pi} I(\vec{r},\vec{s}\,')\Phi(\vec{s}\cdot\vec{s}\,')\,d\Omega' \quad (3)$$

Our current model includes fluid and solid domains and has successfully duplicated experimental results for several of the data points. The ground surface is a square with a 10 m diagonal. The fluid domain is 5 m high and comprised of air encompassing the PV panel. The solid domain for the ground is 6 m thick to match the temperature gradients shown by Reddy [27]. The PV panel is centered in the computational domain 1.5 m above the ground with a tilt angle of 30° from horizontal. It is modeled as a solid domain of silicon, using material properties from the literature. Figure 1 shows the geometry used for the model.

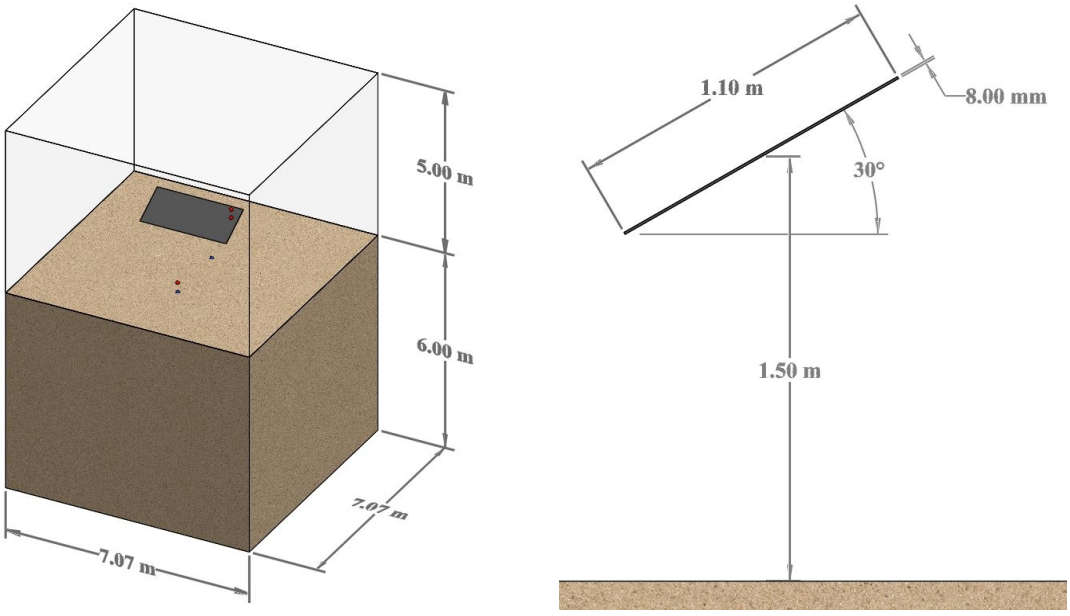

Fig. 1 Model geometry

Some material properties for each of the three domains have been adjusted in order to duplicate the temperatures and fluxes seen in the experiment. These adjustments were to the refractive index for the solids and the absorption coefficient for air. Adjusting the absorption coefficient of air is one method to account for participating media not specifically included in the simulation, such as water vapor or carbon-dioxide. All values were within the ranges of values found in literature. The current values are shown in Table 1.

Table 1. Current model material properties

	Material Properties						Wall Surface Radiation Boundary Conditions	
	Density [kg/m^3]	**Specific Heat** [J/(kg*K)]	**Thermal Conductivity** [W/(m*K)]	**Absorption Coefficient** [1/m]	**Scattering Coefficient** [1/m]	**Refractive Index (n)** [ ]	**Internal Emissivity (ε)** [ ]	**Diffuse Fraction (f_d)** [ ]
Ground	2030	756	1.19	0	0.01	2.5	0.85	0.3
PV Panel	2500	1000	20	0	0.1	3	0.9	0.2
Air	Ideal Gas	1006.43	0.02	0.05	0.05	1	N/A	N/A

Figure 2a shows the mesh, including the fluid (air) domain, the PV panel domain, and the ground domain. Figure 2b shows the mesh within the PV panel domain and the surrounding fluid domain. The mesh solver was set to have finer resolution for boundary layers using an optimized polyhedral configuration. The mesh was defined using mostly face sizing limits, including: 20 mm for the PV panel, 1 m for all of the exterior walls, and 100 mm for the ground surface. An edge sizing of 15 mm was added to the exterior edge of the ground surface. A total of 5 boundary layers were added to all surfaces within the fluid domain. This provided a mesh with an average orthogonal quality of 0.2. The y^+ values for the PV panel surfaces was acceptable with an average of 1.75 and a maximum of 2.5. However, the large face sizing on the ground surface led to less desirable and more varied y^+ values with an average of 5.56 and a maximum of 16.5.

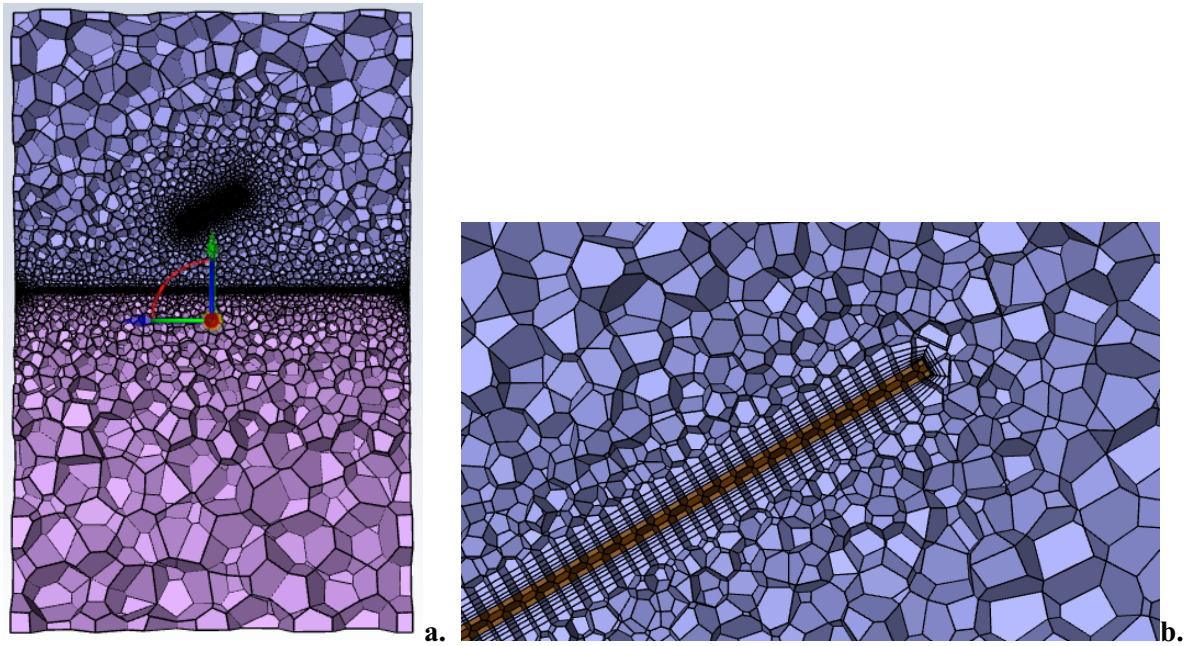

a. **b.**

Fig. 2 Polyhedral mesh for all domains (a) and mesh near PV panel (b)

6. RESULTS

Figure 3 is the resulting temperature contour plot for a steady state simulation of the model set to 1 pm on 25 July 2023. The high-temperature region shown on the ground surface is an artifact of the simulation and the model's solar irradiation setup. This effect is likely due to how the model is treating the radiation at the exterior wall. The affected area is sufficiently far from the measurement locations as to not affect the results. To better understand this non-physical condition, additional simulations were performed. The new simulations used identical conditions with the only variable being the angle of solar radiation. The incident radiation contours are shown in Figure 4. The anomalous edge effect changes with each result. Figure 4a uses the solar angle for 12pm, while figure 4b is at 1pm of the same day. Figure 4c used a solar position of exactly normal to the ground surface.

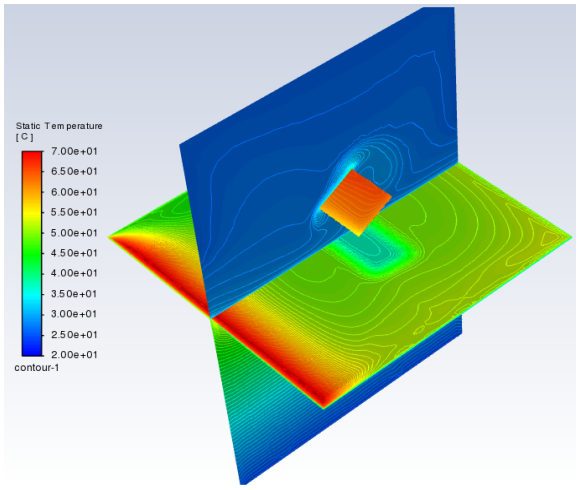

Fig. 3 Temperature contour plot of simulation results

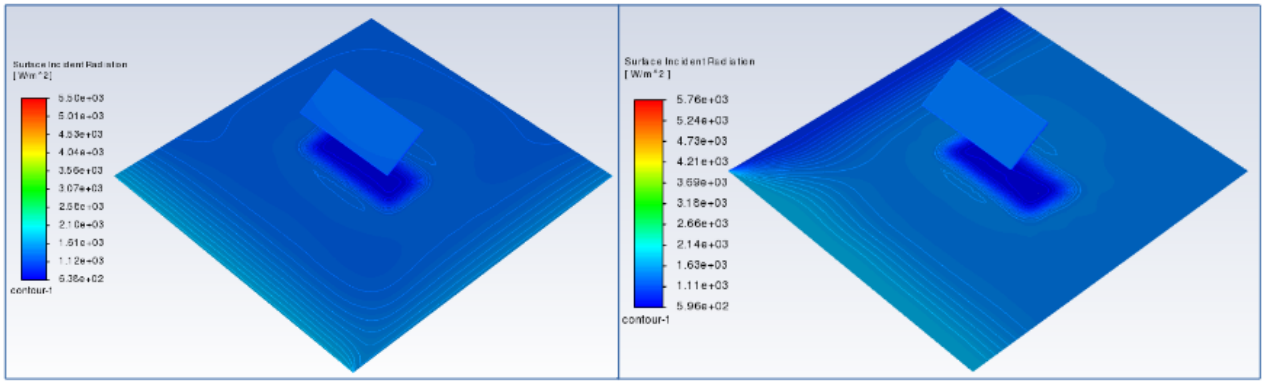

a. 25 July 12pm Cookeville, TN, USA **b.** 25 July 1pm Cookeville, TN, USA

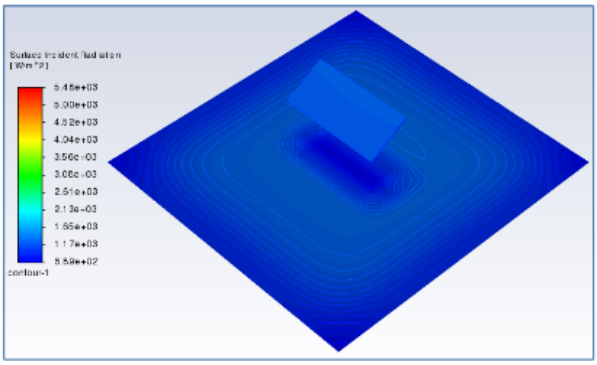

c. Solar radiation artificially set normal to ground surface

Fig. 4 Incident radiation at 3 varied solar angles to demonstrate changes in edge effects

The experimental setup recorded temperatures in several locations with uncertainties for most results between 3 and 4 ˚C depending on the measured value. The air temperatures above the panel had better uncertainty around 0.5 ˚C. Figure 5 shows the locations in the simulation that match the measurement locations in the experimental setup. The shaded and unshaded surface temperatures are measured at the ground surface. The unshaded air temperature is measured 30 cm above the unshaded ground temperature. PV air temperature 1 is 25 cm above the eastern edge of the PV panel. PV air temperature 2 is 25 cm above PV air temperature 1. The PV face and back temperatures were also measured using surface temperature

sensors. The comparison of temperatures from the simulation with temperatures measured experimentally are shown in Table 2.

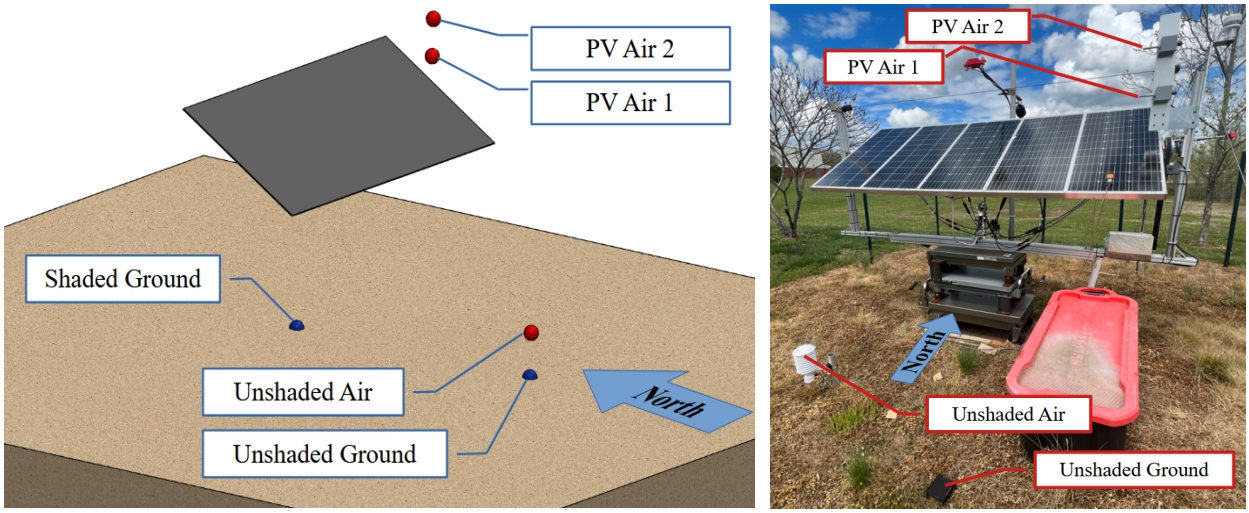

Fig. 5 Single point temperature locations shown in model and experimental setup

Table 2. Experimental data versus simulation data [˚C]

	PV Front Surface	Unshaded Ground	PV Back Surface	Shaded Ground	Unshaded Air	PV Air 1	PV Air 2
Experimental Data	60.14	51.47	60.78	36.75	26.26	38.18	37.96
Simulation Data	63.48	49.27	63.35	37.84	28.57	30.19	28.63

7. CONCLUSIONS

These preliminary results are quite promising with respect to being able to duplicate the experiment with the model. The surface temperatures are within 3.5 ˚C of the experimental results. The PV face temperatures in the simulation are average values over the whole surface, where the experimental values are at points near the edge. This could be a justification for the discrepancy, however these results are within the uncertainty of the measurement. The shaded and unshaded ground temperatures are within 2.2 ˚C of the experimental results. This may be attributed to the non-homogeneity of the actual ground surface of the experiment. While the unshaded air temperatures match fairly well, the air temperatures above the panels do not agree. The experimental results are warmer by 8 ˚C or more. This larger discrepancy could be due to a number of factors. First, the values from the simulation are air temperatures at that point without any influence from radiation. In the experiment, the temperature probes may experience heating from several radiation sources. Second, the air within the simulation does not include any participating gases like carbon dioxide or water vapor. If the air during the experiment was humid, it is likely to take on more heat from the radiation off the PV panel.

REFERENCES

[1] "April 25, 1954: Bell Labs Demonstrates the First Practical Silicon Solar Cell". APS News. 18 (4). American Physical Society. April 2009.
[2] "Solar Industry Data". SEIA. https://www.seia.org/solar-industry-research-data
[3] "Solar Module OEMs Seeking Advantage With Inverter Electronics". Greentech Media. 23 October 2012. https://www.greentechmedia.com/articles/read/Solar-Module-OEMs-Seeking-Advantage-with-Inverter-Electronics

[4] "Statistics about selected locations for utility-scale solar parks". Wiki-Solar. https://www.wiki-solar.org/analysis/norms.html
[5] Barron-Gafford, G. A. et al. The Photovoltaic Heat Island Effect: Larger solar power plants increase local temperatures. Sci. Rep. 6, 35070; doi: 10.1038/srep35070 (2016).
[6] Li Guoqing, Rebecca R Hernandez, George Alan Blackburn, Gemma Davies, Merryn Hunt, James Duncan Whyatt, Alona Armstrong, Ground-mounted photovoltaic solar parks promote land surface cool islands in arid ecosystems, Renewable and Sustainable Energy Transition, Volume 1, 2021, 100008, ISSN 2667-095X, https://doi.org/10.1016/j.rset.2021.100008.
[7] Jubayer, C. M., & Hangan, H. (2014). Numerical simulation of wind effects on a stand-alone ground mounted photovoltaic (PV) system. Journal of Wind Engineering and Industrial Aerodynamics, 134, 56−64. https://doi.org/10.1016/j.jweia.2014.08.008
[8] Jubayer, C. M., & Hangan, H. (2016). A numerical approach to the investigation of wind loading on an array of ground mounted solar photovoltaic (PV) panels. Journal of Wind Engineering and Industrial Aerodynamics, 153, 60−70. https://doi.org/10.1016/j.jweia.2016.03.009
[9] Irtaza, H., & Agarwal, A. (2018). CFD Simulation of Turbulent Wind Effect on an Array of Ground-Mounted Solar PV Panels. Journal of the Institution of Engineers (India). Series A, Civil, Architectural, Environmental and Agricultural Engineering, 99(2), 205−218. https://doi.org/10.1007/s40030-018-0283-x
[10] Lee, G.-H., Choi, J.-W., Kim, J., Seo, J.-H., & Ha, H. (2021). Numerical simulations of wind loading on the floating photovoltaic systems. Journal of Visualization, 24(3), 471−484. https://doi.org/10.1007/s12650-020-00725-z
[11] Jubayer, C. M., & Hangan, H. (2016). A numerical approach to the investigation of wind loading on an array of ground mounted solar photovoltaic (PV) panels. Journal of Wind Engineering and Industrial Aerodynamics, 153, 60−70. https://doi.org/10.1016/j.jweia.2016.03.009
[12] Chowdhury, M. G., Goossens, D., Goverde, H., & Catthoor, F. (2018). Experimentally validated CFD simulations predicting wind effects on photovoltaic modules mounted on inclined surfaces. Sustainable Energy Technologies and Assessments, 30, 201−208. https://doi.org/10.1016/j.seta.2018.10.005
[13] Abdullah, A. L., Misha, S., Tamaldin, N., Rosli, M. A. M., & Sachit, F. A. (2019). Numerical analysis of solar hybrid photovoltaic thermal air collector simulation by ANSYS. CFD Letters, 11(2), 1-11.
[14] Kasaeian, Alibakhsh, Yasamin Khanjari, Soudabeh Golzari, Omid Mahian, and Somchai Wongwises. (2017) Effects of forced convection on the performance of a photovoltaic thermal system: An experimental study. Experimental Thermal and Fluid Science 85, 13-21.http://dx.doi.org/10.1016/j.expthermflusci.2017.02.012
[15] Wu, Y.-Y., Wu, S.-Y., & Xiao, L. (2017). Numerical study on convection heat transfer from inclined PV panel under windy environment. Solar Energy, 149, 1−12. https://doi.org/10.1016/j.solener.2017.03.084
[16] Naghavi, M. S., Esmaeilzadeh, A., Singh, B., Ang, B. C., Yoon, T. M., & Ong, K. S. (2021). Experimental and numerical assessments of underlying natural air movement on PV modules temperature. Solar Energy, 216, 610−622. https://doi.org/10.1016/j.solener.2021.01.007
[17] Alblawi, A., & Talaat, M. (2022). Experimental and Simulation Study Investigating the Effect of a Transparent Pyramidal Cover on PV Cell Performance. Sustainability (Basel, Switzerland), 14(5), 2599-. https://doi.org/10.3390/su14052599
[18] Poruba, A., Fejfar, A., Remeš, Z., Špringer, J., Vaněček, M., Kočka, J., Meier, J., Torres, P., & Shah, A. (2000). Optical absorption and light scattering in microcrystalline silicon thin films and solar cells. Journal of Applied Physics, 88(1), 148−160. https://doi.org/10.1063/1.373635
[19] Oh, J., Rammohan, B., Pavgi, A., Tatapudi, S., Tamizhmani, G., Kelly, G., & Bolen, M. (2018). Reduction of PV Module Temperature Using Thermally Conductive Backsheets. IEEE Journal of Photovoltaics, 8(5), 1160−1167. https://doi.org/10.1109/JPHOTOV.2018.2841511
[20] Wang, J., Nilsson, A. M., Barrios, D., Vargas, W. E., Wäckelgård, E., & Niklasson, G. A. (2020). Light scattering materials for energy-related applications: Determination of absorption and scattering coefficients. Materials Today : Proceedings, 33(Part 6), 2474−2480. https://doi.org/10.1016/j.matpr.2020.01.339
[21] Zhang, B., Han, C., & Yu, X. (Bill). (2015). A non-destructive method to measure the thermal properties of frozen soils during phase transition. Journal of Rock Mechanics and Geotechnical Engineering, 7(2), 155−162. https://doi.org/10.1016/j.jrmge.2015.03.005
[22] Singh, R. K., & Sharma, R. V. (2017). Numerical analysis for ground temperature variation. Geothermal Energy (Heidelberg), 5(1), 1−10. https://doi.org/10.1186/s40517-017-0082-z
[23] Li, P., Guo, F., & Yang, X. (2022). An inversion method to estimate the thermal properties of heterogeneous soil for a large-scale borehole thermal energy storage system. Energy and Buildings, 263, 112045-. https://doi.org/10.1016/j.enbuild.2022.112045
[24] Ahmad Vasel, Frantzis Iakovidis, (2017) The effect of wind direction on the performance of solar PV plants. Energy Conversion and Management, Volume 153, Pages 455-461.
[25] Cannon, D.T. & Vasel-Be-Hagh, A. (2024). Daytime Thermal Effects of Solar Photovoltaic Systems: Field Measurements. Journal of Renewable and Sustainable Energy (in press).
[26] Fluent Inc. (2024). Fluent 2023 R2 Theory Guide
[27] G. B. Reddy (2000) An experimental investigation of subsurface ground temperature in Texas: a complete study, International Journal of Ambient Energy, 21:4, 196-202, http://dx.doi.org/10.1080/01430750.2000.967537